

# Impact of the Angular Velocity on the Signals Spectrum and Performance of Antenna-Array Receivers

Mamadou Abdoulaye Diop, Karim Cheikhrouhou, and Sofiène Affes  
INRS-ÉMT, Université du Québec, Montreal, Canada  
{diop,cheikhro,affes}@emt.inrs.ca

**Abstract**— Tremendous effort was previously made to estimate the location of moving sources with large angular velocities. However, to the best of our knowledge, no previous work has thoroughly investigated the effect of the combined angular velocity and mobile speed on the spectrum of the signal received by an antenna-array. In this contribution, we address this issue in the particular context of wideband CDMA transmission. We first show both by theoretical development and by simulations that the maximum frequency shift is the sum of the conventional Doppler term and a new term due to angular speed and that it is a linear function of both. We also show that the additional frequency shift due to the angular speed increases channel identification errors and thereby degrades the performance of antenna-array receivers. This performance loss becomes even higher at a larger number of antennas in the array.

## I. INTRODUCTION

Many research efforts were spent to address the problem of time-varying direction of arrival (DOA). Most of these studies concentrated on evaluating the localization of sources which have significant angular velocities [1], [2]. However, to the best of our knowledge, no previous work has thoroughly investigated the effect of the combined angular velocity and mobile speed on the spectrum of the signal received by an antenna-array. In this contribution, we address this issue in the particular context of wideband transmission using antenna-array receivers.

To carry out this study, we consider propagation in a selective Rayleigh-fading multipath environment. The conventional power spectrum density (PSD) derivation was provided in details in the seminal work by Jakes [3]. It was shown there that the maximum frequency shift of the PSD corresponds to the Doppler shift. Derivation of a closed-form expression for the maximum frequency shift of the PSD when the mobile has a constant speed and significant angular velocity represents one of the contributions of this paper. Evaluations by simulations of the PSD show that the theoretical and simulated maximum frequency shift are almost identical. This result confirms, first, that the conventional Doppler term and the term due to angular speed are additive. Second, it suggests that the maximum frequency shift is a linear function of the angular speed.

Additionally, another contribution of this paper in an assessment of the impact of time-varying DOA on WCDMA

receivers performance in terms of channel identification error. Numerical results show an important degradation of the receiver performance. This loss becomes even higher at a larger number of antennas in the array [6].

## II. DATA AND TIME-VARYING DOA MODELS

We consider a single-user receiver structure on the uplink direction (portable-to-base station) of a cellular wideband CDMA system. Let us assume that each base station is equipped with  $M$  receiving antennas. We consider  $P$  propagation paths in a selective fading multipath environment. The user's binary phase shift keying bit sequence is first differentially encoded as  $b_n = \underline{b}_n b_{n-1}$  at a rate  $1/T_s$ , where  $T_s$  is the bit duration.

After despreading the data sequence at the receiver side, we form for each path  $p = 1, \dots, P$  the corresponding  $M \times 1$  despread vector:

$$\mathbf{Z}_{p,n} = G_{p,n} \varepsilon_{p,n} \psi_n b_n + N_{p,n}, \quad (1)$$

where  $\psi_n^2$  is the total received power and  $\varepsilon_{p,n}^2$  is the normalized power fraction of the total power received over the  $p$ -th multipath (*i.e.*,  $\sum_{p=1}^P \varepsilon_{p,n}^2 = 1$ ). The  $M \times 1$  vector  $G_{p,n} = [g_{p,1,n}, \dots, g_{p,m,n}, \dots, g_{p,M,n}]^T$ , with norm  $\sqrt{M}$ , denotes the channel vector from the transmitter to the multi-antenna receiver over the  $p$ -th multipath.

For more efficient joint space-time processing, the  $M \times 1$  vectors  $G_{p,n}$  are aligned to generate the following  $MP \times 1$  data observation vector:

$$\mathbf{Z}_n = [\mathbf{Z}_{1,n}^T, \dots, \mathbf{Z}_{P,n}^T]^T = \underline{\mathbf{H}}_n s_n + \underline{\mathbf{N}}_n, \quad (2)$$

where  $s_n = \psi_n b_n$  denotes the signal component,  $\underline{\mathbf{H}}_n = [\varepsilon_{1,n} G_{1,n}, \dots, \varepsilon_{P,n} G_{P,n}]$  is the  $MP \times 1$  space-time channel vector with norm  $\sqrt{M}$ .  $\underline{\mathbf{N}}_n = [N_{1,n}^T, \dots, N_{P,n}^T]^T$  is a space-time uncorrelated Gaussian interference vector with mean zero and variance  $\sigma_N^2$  after despreading of the data channel. The resulting input SNR after despreading is  $SNR_{in} = \frac{\psi_n^2}{\sigma_N^2}$  per antenna element.

The vector channel  $G_{p,n}$  is considered as a superposition of propagation path contributions associated to a continuum of angles of arrival (AOA)  $\theta$ , propagation delays  $\tau$  and Doppler angles  $\phi$  [7].

Considering a linear antenna array and for an angular spread  $\Delta\theta = 0$ , the propagation follows a plane wave with

a specified direction of arrival  $\theta_{p,n}$ . The channel vector  $G_{p,n}$  could be written as follows:

$$G_{p,n} = r_{p,n} F(\theta_{p,n}), \quad (3)$$

where  $r_{p,n}$  is a phase shift due to Rayleigh fading and  $F(\theta)$  is the array propagation vector, defined as:

$$F(\theta) = \left[ 1, e^{-2j\pi \sin(\theta) \frac{x_1}{\lambda}}, \dots, e^{-2j\pi \sin(\theta) \frac{x_M}{\lambda}} \right]^T, \quad (4)$$

where  $\lambda$  is the wavelength, and  $x_m$ ,  $m = 1, \dots, M$ , are the sensor positions of a linear antenna array ULA.

In this paper, we assume that the DOA in (4) is time-varying. We model the source motion by taking the Taylor series expansions of  $\theta(t + nT_s)$  as follows [1], [2]:

$$\theta(t + nT_s) = \theta(t) + \dot{\theta}nT_s + \ddot{\theta}(nT_s)^2/2 + \dots \quad (5)$$

Let us consider a time-varying DOA environment in which the first-order polynomial approximation of the DOA realization is assumed. Therefore, the time variable DOA is postulated as [4]:

$$\theta_{p,n} = \theta_{p,0} + \dot{\theta}nT_s, \quad (6)$$

where  $\theta_{p,n}$  is the DOA of the  $p$ -th wave at the sampling instant  $nT_s$ . The initial direction of arrival  $\theta_{p,0}$  is assumed to be uniformly distributed over  $[-\pi, \pi]$ .

### III. IMPACT OF THE TIME-VARYING DOA ON THE SPECTRUM WIDTH

Let  $x_m$  denote the position of the  $m$ -th antenna and  $\lambda$  the wavelength. We show that the PSD  $S_g^m(f)$  of  $g_{p,m,n} = r_{p,n} e^{-2j\pi \sin(\theta_{p,n}) \frac{x_m}{\lambda}}$  is as follows:

$$S_g^m(f) = \sum_{l=-\infty}^{l=+\infty} \sum_{k=-\infty}^{k=+\infty} S \left( f + \frac{l\dot{\theta}}{2\pi} + \frac{k}{T_s} \right) J_l^2 \left( 2\pi \frac{x_m}{\lambda} \right). \quad (7)$$

Equation (7) shows that the RF spectrum of  $g_{p,m,n}$ ,  $S_g^m(f)$ , is an infinite sum of replicas of the Rayleigh spectrum  $S(f)$  (see [3] for details), modulated in amplitude by  $J_l^2(2\pi \frac{x_m}{\lambda})$ . These replicas are shifted in frequency by multiples of  $1/T_s$  and  $l\dot{\theta}/(2\pi)$ . The maximum frequency shift is then obtained as follows:

$$f_{\max} = f_D + |l_0| \frac{\dot{\theta}}{2\pi}, \quad (8)$$

where  $l_0$  is the index of the Bessel function such that  $|J_l(2\pi \frac{x_m}{\lambda})|$  is maximum.

It is worth noting first that the maximum frequency shift  $f_{\max}$  has a close dependency on the antenna position  $x_m$ . Second, the maximum frequency shift  $f_{\max}$  on each antenna is the sum of the conventional Doppler term  $f_D$  and a new one  $f_\theta$  due to the angular speed which is given by:

$$f_\theta = |l_0| \frac{\dot{\theta}}{2\pi}. \quad (9)$$

The angular speed should satisfy the following condition:

$$\dot{\theta} < \dot{\theta}_{\max} = \frac{\pi}{|l_0|} \left( \frac{1}{T_s} - 2f_D \right), \quad (10)$$

otherwise the channel will be quasi-uncorrelated, the base-band PSD being formed by multiple and independent rays over  $[-\frac{1}{2T_s}, \frac{1}{2T_s}]$  in this case.

## IV. VALIDATION AND EVALUATION BY SIMULATIONS

### A. Maximum frequency shift validation

In this section, we validate by simulations the theoretical derivations of the power spectrum density and the maximum frequency shift developed in the previous section.

For this purpose, we use the channel model in [3] to generate  $P = 3$  equal-power Rayleigh-fading channel coefficients. Initial DOA values for these paths are  $\theta_{1,0} = \pi/7$ ,  $\theta_{2,0} = -\pi/5$  and  $\theta_{3,0} = -\pi/3$ . At the receiver, we consider  $M = 8$  or 16 antenna elements of a uniform linear array (ULA). In this part of study, transmission is assumed noise-free.

The position  $x_m$  of an antenna element in a uniform linear array is defined as:  $x_m = [+M/2, \dots, -M/2]$ ,  $m = 1, \dots, M$ .

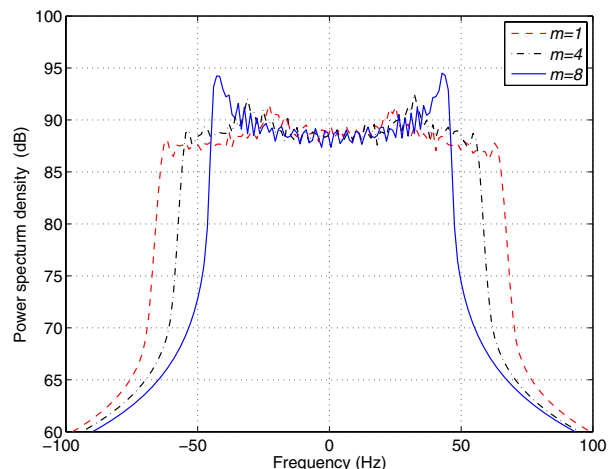


Fig. 1. Simulated PSD for different antenna positions  $m$  at  $\dot{\theta} = 3 \times 10^{-4}$  rad/sym with a ULA of  $M = 16$  sensors and  $v = 25$  Km/h.

In Figs. 1 and 2, we provide the PSD for different antenna positions and angular speeds, respectively, at a constant vehicular speed  $v = 25$  Km/h. The results suggest the following:

- For an antenna position close to the center of the ULA, the shift in frequency is very close to  $f_D$ . Indeed,  $f_\theta$  still affects the whole system but in this specific position, it has a negligible value (around 1 Hz for  $\dot{\theta} = 3 \times 10^{-4}$  rad/sym) compared to  $f_D = 45$  Hz.
- Moving left or right to either end of the ULA, the frequency shift  $f_\theta$  due to the presence of  $\dot{\theta}$  increases significantly. At the first position  $x_m = M/2$ , it has

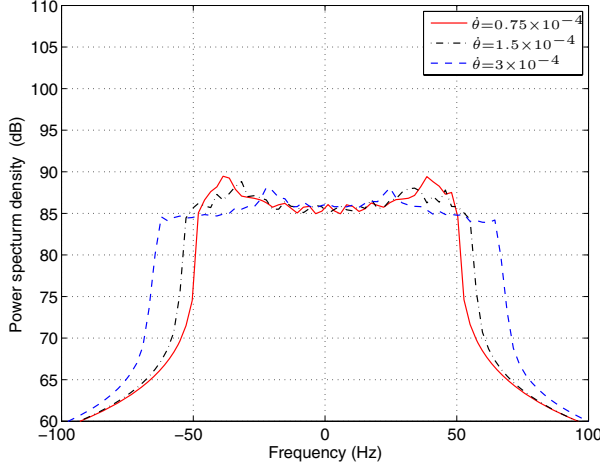


Fig. 2. Simulated PSD for different angular speeds  $\dot{\theta}$  at antenna position  $m = 1$  with a ULA of  $M = 16$  sensors and  $v = 25$  Km/h.

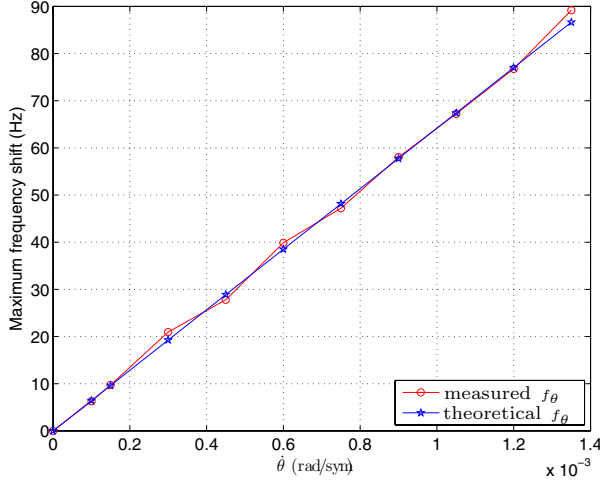


Fig. 3. Maximum frequency shift versus angular speeds  $\dot{\theta}$  at  $v = 0$  Km/h for the antenna position  $m = 1$  of a ULA of  $M = 16$  sensors.

a maximum value of about 20 Hz compared to 8 Hz, for  $x_m = M/4$  or 1 Hz for  $x_m = 1$ .

Derivation of the closed-form expressions for the maximum frequency shift in (8) and  $f_\theta$  in (9) are one of the two key contributions of this paper. To validate by simulations these results, we adopt the following strategy: first we set the mobile speed  $v$  to 0 Km/h to eliminate the Doppler effect, *i.e.*,  $f_D = 0$  Hz. We then plot in Figs. 3 and 4 both the theoretical and simulated maximum frequency shifts for different angular speeds and different indexes  $l_0(x_m)$  that maximize the Bessel function  $J_l^2(2\pi \frac{x_m}{\lambda})$ . These figures show almost identical theoretical and simulated results.

Second, we had to demonstrate that the conventional Doppler term and the one due to angular speed are additive and that the maximum frequency shift has a linear relationship with both terms. We plot in Fig. 5 the measured maximum spectrum shift versus the angular speed  $\dot{\theta}$  at 0, 25 and 50 Km/h, resulting in a Doppler shift

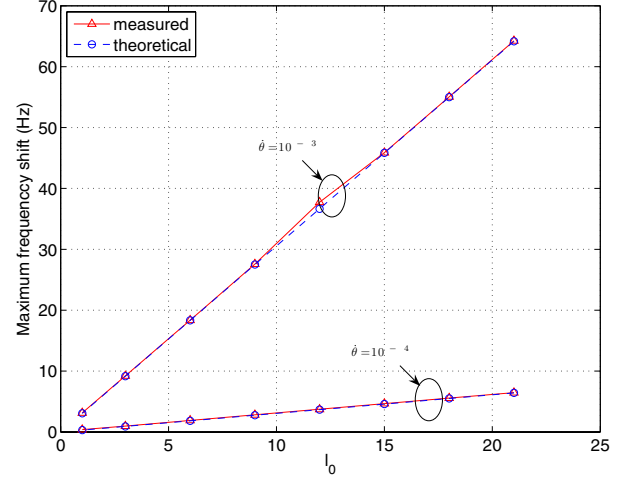


Fig. 4. Maximum frequency shift versus  $l_0$  at  $v = 0$  Km/h for a ULA of  $M = 16$  sensors.

$f_D$  of about 0, 45, and 90 Hz, respectively. This figure confirms first that  $f_{\max}$  is a linear function of the angular speed  $\dot{\theta}$  like what was suggested by (8). Besides, it shows that the frequency difference between curves at  $v = 25$  Km/h,  $v = 50$  Km/h and the curve at  $v = 0$  Km/h for all values of  $\dot{\theta}$  represents the Doppler term  $f_D$ . This result confirms that both terms are additive.

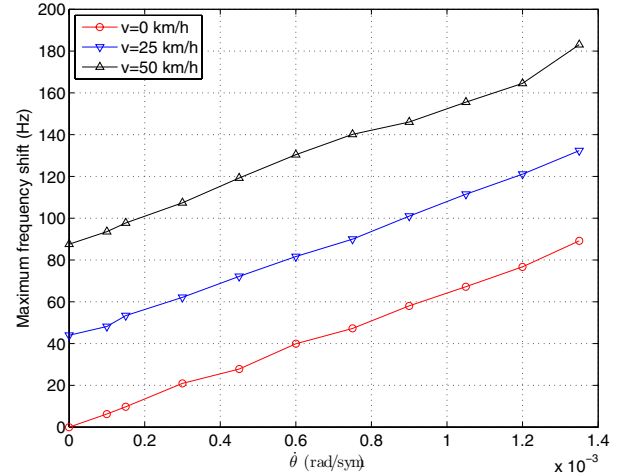


Fig. 5. Maximum frequency shift versus angular speed  $\dot{\theta}$  for the antenna position  $m = 1$  of a ULA of  $M = 16$  sensors.

On the other hand, if the angular speed is close to a limit  $\dot{\theta}_{\max}$  value for a fixed element position, the additive impact on the spectrum of the angular speed disappears. In this case, we notice the existence of various dominating rays. Hence, the resulting spectrum appears as that of a quasi-uncorrelated channel.

The condition over  $\dot{\theta}$  established in (10) is plotted in Fig. 6 and compared to measured  $\dot{\theta}_{\max}$ . This value is obtained whenever the spectrum shows independent rays. The small difference between curves shows that the approximation

and simplification made to derive  $\dot{\theta}_{\max}$  is acceptable.

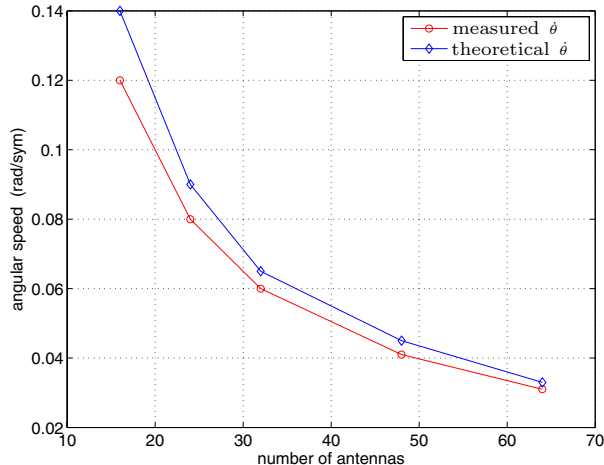


Fig. 6. Measured and theoretical angular velocity limit  $\dot{\theta}_{\max}$ .

### B. Impact of the angular speed on the performance of WCDMA antenna-array receivers

1) *Overview of the tested receiver:* To carry out this part of this contribution, we selected the spatio-temporal array-receiver [5] as a common array-processing core structure. At iteration  $n$ , this blind array receiver uses the channel estimate  $\hat{\mathbf{H}}_n$  to extract the data signal component by spatio-temporal MRC:

$$\hat{s}_n = \text{Re} \left\{ \frac{\hat{\mathbf{H}}_n^H \mathbf{Z}_n}{M} \right\}. \quad (11)$$

The DBPSK data sequence  $b_n$  is then estimated as  $\hat{b}_n = \text{sign}\{\hat{s}_n\}$ . The receiver feeds back the estimate of the data signal component  $\hat{s}_n$  (or  $\hat{\psi}_n \hat{b}_n$ ) in a decision feedback identification (DFI) scheme to update the channel estimate as follows:

$$\hat{\mathbf{H}}_{n+1} = \hat{\mathbf{H}}_n + \mu (\mathbf{Z}_n - \hat{\mathbf{H}}_n \hat{s}_n) \hat{s}_n, \quad (12)$$

where  $\mu$  is the adaptation step-size. This DFI scheme identifies the channel within a constant sign ambiguity  $a = \pm 1$ , thereby giving  $\hat{\mathbf{H}}_n \simeq a \mathbf{H}_n$  and  $\hat{b}_n \simeq a b_n$ . However, differential decoding of  $\hat{b}_n$  resolves the sign ambiguity in the BPSK symbol estimates  $\hat{b}_n = \hat{b}_n \hat{b}_{n-1}$ .

The total power received from the desired user is estimated for power control by:

$$\hat{\psi}_n^2 = (1 - \alpha) \hat{\psi}_{n-1}^2 + \alpha |\hat{s}_n|^2, \quad (13)$$

where  $\alpha \ll 1$  is a smoothing factor, while the bit sequence  $\hat{b}_n$  is estimated from the sign of  $\hat{s}_n$ .

In this paper, we define the channel misadjustment as the mean square error per diversity branch of channel identification in both space and time as:

$$\beta^2 = \frac{\text{E} [\|\Delta \mathbf{H}_n\|^2]}{MP} = \frac{\text{E} [\|\hat{\mathbf{H}}_n - \mathbf{H}_n\|^2]}{MP} \quad (14)$$

2) *Simulation setup:* We consider a wireless channel characterized by  $P = 3$  equal power Rayleigh fading paths propagating from directions with time varying DOAs. Each mobile transmits a BPSK data sequence received by a uniform linear array (ULA) of  $M = 8$  or 16 antenna elements. Two representative mobile speeds of almost 5 and 25 km/h resulting in a Doppler shift of about 9 and 45 Hz, respectively at a carrier frequency of  $f_c = 1.9$  GHz are examined. Power control (PC) requests an incremental change of  $\pm 0.625$  dB in transmitted power every 0.625 ms and an error of 10% over the PC bit command.

An analytical expression for the optimum step-size  $\mu$  was previously derived in [6]. Its expression provides a minimum channel estimation misadjustment using the DFI scheme [5].

3) *Simulation results:* In Figs. 7 and 8, we plot the identification error versus the input SNR in dB for both mobile speeds of  $v = 5$  Km/h and  $v = 25$  Km/h.

We plot curves for  $\dot{\theta} = 0$ ,  $\dot{\theta} = 3 \times 10^{-4}$  and  $\dot{\theta} = 3 \times 10^{-3}$  rad/sym, resulting in a maximum frequency shift (at the antenna position  $x_m = M/2$ ) of about  $f_\theta = 0$ ,  $f_\theta = 8.3$  and  $f_\theta = 83$  Hz, respectively, for  $M = 8$  and  $f_\theta = 0$ ,  $f_\theta = 19.3$  and  $f_\theta = 193$  Hz, respectively, for  $M = 16$  sensors.

Results suggest the following:

- At a reduced mobile speed of  $v = 5$  Km/h, a loss of about 0.5 and 5.5 dB in identification error is measured at an angular speed of  $\dot{\theta} = 3 \times 10^{-4}$  and  $\dot{\theta} = 3 \times 10^{-3}$  rad/sym, respectively. This is due to the sole effect of angular speed which is more important in the case of  $\dot{\theta} = 3 \times 10^{-3}$  rad/sym where the frequency shift is about 10 times larger for  $\dot{\theta} = 3 \times 10^{-4}$  rad/sym. The loss increases with more antennas due to the increase of  $f_\theta$  from 8.3 to 83 Hz for  $M = 8$  and from 19.3 to 193 Hz for  $M = 16$ .
- The angular speed at  $\dot{\theta} = 3 \times 10^{-4}$  has a negligible impact on the receiver identification error at a mobile speed  $v = 25$  Km/h. Whatever is the value of the SNR, the gap between curves at  $\dot{\theta} = 0$  and  $\dot{\theta} = 3 \times 10^{-4}$  remains negligible. At a higher mobile speed, the impact of the angular speed becomes negligible on receiver identification. We can see a noticeable degradation in the identification error only for a large ULA.
- Overall, the performance degradation in terms of identification error of the receiver due to the angular speed is even higher when the mobile speed is slow. Besides, it depends mainly on the number of antennas in the ULA. Therefore, when considering an increase in the number of antenna elements as a solution to any antenna-receiver performance improvement, a tradeoff should be made between losses in identification accuracy and capacity or spectrum efficiency enhancement. This result provides a new insight into antenna-array receiver design.

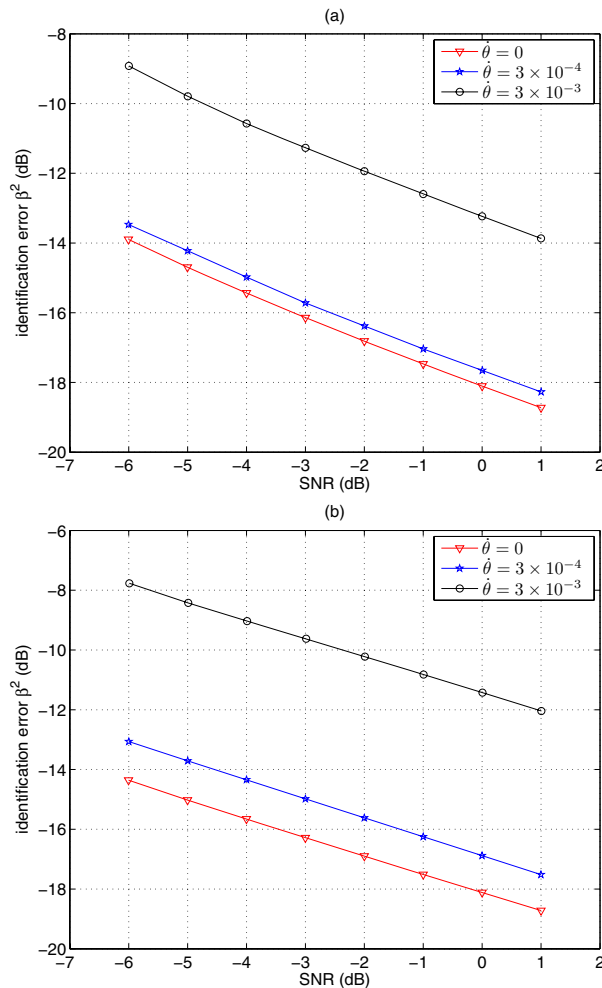


Fig. 7. Identification error vs SNR (dB) for different angular speeds at  $v = 5$  Km/h with (a):  $M = 8$  and (b):  $M = 16$  sensors.

## V. CONCLUSIONS

In this paper, the effect of the combined angular velocity and mobile speed on the spectrum of the signal received by an antenna-array has been investigated in the particular context of wideband CDMA transmission. By either theoretical development and simulations it was shown that the maximum frequency shift is the sum of the conventional Doppler term and a new term due to angular speed and that it is a linear function of both. Additionally, it was also shown that the additional frequency shift due to the angular speed increases channel identification errors and thereby degrades the performance of antenna-array receivers. This performance loss becomes even higher at a larger number of antennas in the array.

## ACKNOWLEDGMENT

This work is supported by a Canada Research Chair in High-Speed Wireless Communications and the Strategic Partnership Projects Program of NSERC.

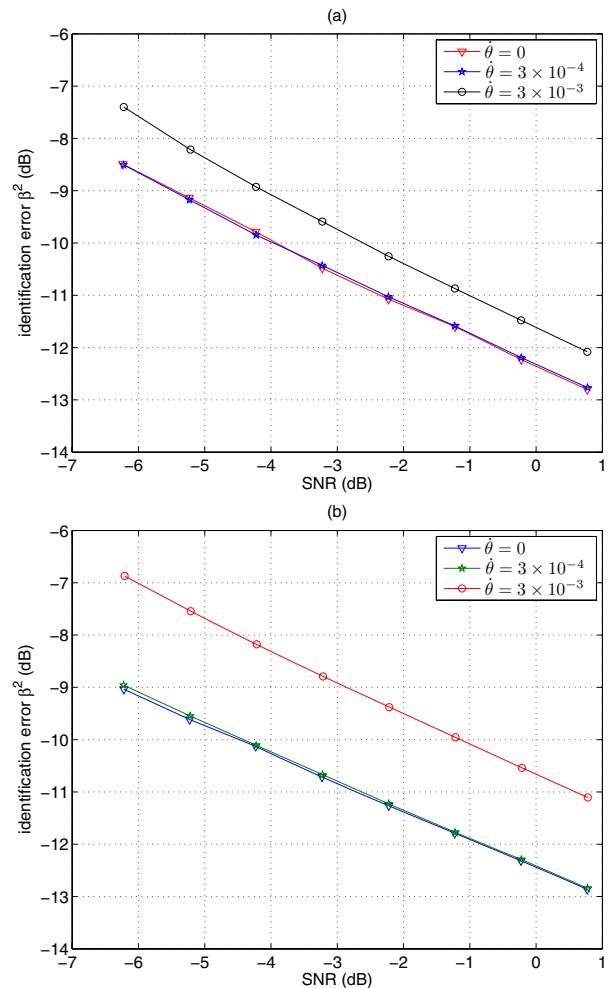


Fig. 8. Identification error vs SNR (dB) for different angular speeds at  $v = 25$  Km/h with (a):  $M = 8$  and (b):  $M = 16$  sensors.

## REFERENCES

- [1] V. Katkovnik and A. B. Gershman, "Performance study of the local polynomial approximation based beamforming in the presence of moving sources", *IEEE Trans. Ant. Prop.*, vol. 50, no. 8, pp. 1151-1157, Aug. 2002.
- [2] W. Montlouis, O. Bayat and B. Shafai, "DOA and angular velocity estimation using planar array with subspace based initialization", *IEEE Milcom*, vol. 5, pp. 2797- 2801, Oct. 2005.
- [3] W. C. Jakes and Ed., *Microwave Mobile Communications*, John Wiley & Sons, 1974.
- [4] T. Wigren and A. Eriksson, "Accuracy aspects of DOA and angular velocity estimation in sensor array processing", *IEEE Signal Processing Lett.*, vol. 2, no. 4, pp. 60-62, Apr. 1995.
- [5] S. Affes and P. Mermelstein, "A new receiver structure for asynchronous CDMA: STAR - the spatio-temporal array receiver", *IEEE Journal on Selected Areas in Communications*, vol. 16, no. 12, pp. 1411-1422, October 1998.
- [6] M. A. Diop, "Impact of the angular spread and the angular velocity on the performance of new 3G+ antenna-array receivers", MSc Thesis (in French), INRS-EMT (Institut Nationale de la Recherche Scientifique, Energie, Matériaux et Télécommunications), Montréal, Québec, Canada, 2006.
- [7] A. Stéphanne and B. Champagne, "Effective multi-path vector channel for antenna arrays systems", *IEEE Transactions on Vehicular Technology*, vol. 49, no. 6, pp. 2370-2381, November 2000.